

Stress distribution in polymeric film laminated leather under biaxial loading

Virginija Jankauskaitė, Eugenija Strazdienė and Agnė Laukaitienė

Department of Clothing and Polymer Products Technology, Kaunas University of Technology, Studentu str. 56, LT-51424 Kaunas, Lithuania; virginija.jankauskaite@ktu.lt

Received 24 October 2005, in revised form 4 May 2006

Abstract. The needle and stitch parameters on pigment-coated and polymeric film laminated leather behaviour under biaxial loading have been investigated. Simulation by finite element analyses (FEA) was used to determine the influence of the stitch number upon the distribution of principal stresses under the membrane deformation, while by experiments punching of the investigated materials was performed using a special punching unit. Investigations by FEA show that the stress in the middle of a stitch is four to five times higher than stresses at the beginning or at the end of the stitch. Besides, the increase of the stitch density increases stress values. Leather and polyurethane film break up straight below the specimen and punch contact zone. On the other hand, crack formation and propagation depend on the stitch density and shape of the needle.

Key words: laminated leather, biaxial deformation, stress distribution, punching strength.

1. INTRODUCTION

Physical and mechanical properties of leather can be varied depending on the applications (footwear, gloves, clothing, purses, furniture upholstery, saddles, etc.). It is required that leather must be very soft, thin and extensible for gloves and clothing, more rigid for footwear, hard and stiff for soles, etc.

Generally, after dyeing leather is subjected to finishing in order to improve its wear properties in general and to protect it from wetting and soiling, to level out patches and grain faults, to apply an artificial grain layer to splits or corrected grain leathers and to modify the surface properties (shade, luster, handle, etc.) [1,2]. For this purpose various finishing materials (casein, nitrocellulose, polyurethane, acrylic, other resin and polymer compositions) and techniques (glazing, plating, embossing, spraying and curtain coating finish) can be used [2,3].

In the case of pigment coating, tanned leather is first colored with a penetrating dye. The dye penetrates the surface of the leather giving it colour, but not covering over natural markings. Then leather can be finished in one or more coating operations with clear or pigmented finishes that do not penetrate the surface [3]. Pigment coat imparts the desired appearance of the leather and levels out the surface. Generally, the more finish leather has, the stiffer it becomes. Usually coating thickness does not exceed 0.15 mm.

The other, rarely used, method is to form leather coating by laminating a polymeric film to its surface. In this case the film is made to adhere to the surface by hot pressing with plate [2]. Laminated leather is real leather with a unique microporous finish, allowing breathing more naturally in comfort and providing a layer of protection, which guards against scuffs stain and water. Microporous polyurethane (PU) film is perforated with tiny microscopic holes or pores approximately from 1 to 5 μm in diameter [4]. Water droplets are too large to penetrate the pores in the film and therefore the film is waterproof. Water vapour, generated by the body perspiration, is much smaller (typically less than 0.0003 μm) and passes easily through the holes, carrying moisture away.

The load-elongation and recovery behaviour of leather show considerable differences due to the differences in the structure [5-7]. Especially, differences in the long-term properties show up in the case of laminated leather due to the rearrangement and reorientation at the interface between layers [7,8]. As coated and laminated materials are increasingly used, it is important to understand their behaviour during deformation. Product quality and shape stability highly depend upon cracks location and their formation processes.

In the manufacture of leather garments, their components are often stitched. During the stitch formation process, the sewing needle performs several functions: pinks through material, pulls through it the top thread and capacitates the formation of the thread loop, which later is caught by the nose of the shuttle or looper. Therefore, the requirements for needle quality, strength, precision, geometrical shape and other parameters are very high. The quality of stitches, seams and products in large scale depend on the needle parameters and their conformity to the stitched leather properties. The force of leather perforation, the disturbance of material or threads and heat of the needle are affected by the shape of the needle spike. These factors significantly influence wear properties and the esthetical view of footwear or other products made from leather.

In this report, the influence of needle shape and prick number upon stress distribution of pigment-coated and laminated leather under biaxial loading has been investigated.

2. EXPERIMENTAL

Nappa leather – soft and thin leather, which can be applied for manufacturing of footwear, gloves and clothes – was used (obtained from Joint Stock Company

“Siauliu stumbro odos”, Lithuania). The leather surface was coated with opaque pigmented acrylic emulsion by spraying with compressed air [9]. Depending on the hide quality and requirements, full grain pigmented leather or corrected grain pigmented leather with solid top layer was obtained (Fig. 1a). The pigment coat imparts the desired appearance of the leather and levels out the surface. After pigment coating a topcoat with acrylic lacquer layer was used. The topcoat determines the final appearance of the leather surface and has decisive influence on the fastness properties of the finish. The structure of used pigment finished leather is presented in Fig. 1a.

Laminated leather – *Permair* leather – used in these studies is a commercial grade product (Joint Stock Company “Siauliu stumbro odos”, Lithuania). Such leather is obtained by hot pressing of the microporous polyurethane membrane to split the leather surface. This film, named *Permair*, was manufactured by Porvair International Limited, United Kingdom and supplied in a roll. Bonding of the film was performed by a water-born polyurethane adhesive [7]. Polymeric film provides protection against scuffs, stains and water. The structure of laminated leather is shown in Fig. 1b.

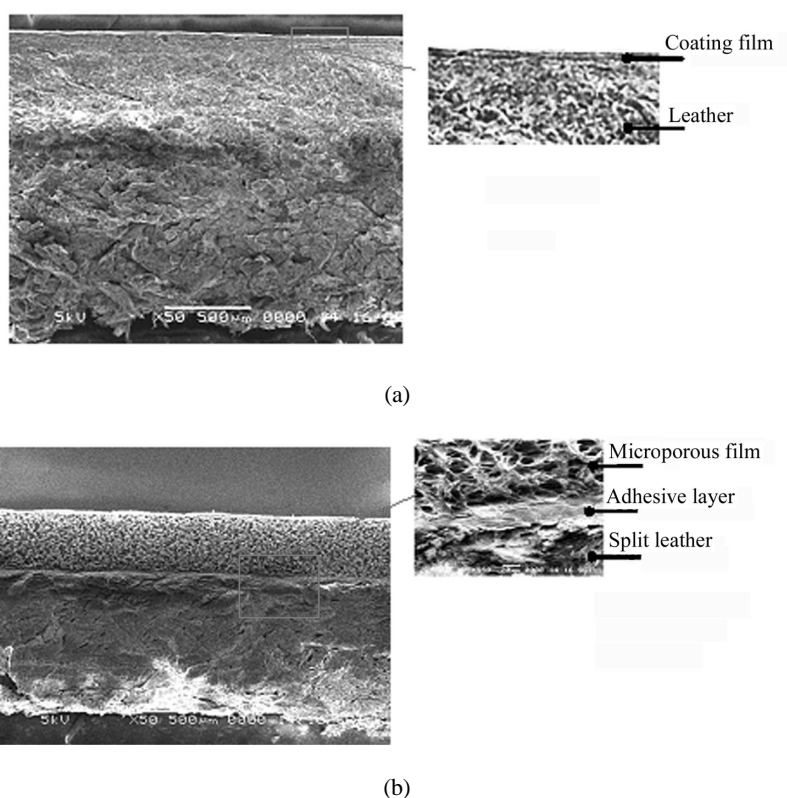


Fig. 1. Structure of pigment coated leather (a) and microporous film laminated leather (b).

Mechanical properties of the coated and laminated leathers used for these investigations are presented in Table 1. Additionally, microporous polyurethane film *Permair* was investigated. It makes about 1/3 of the laminated leather thickness and, therefore, significantly influences its strength and deformation behaviour [7,8].

For these investigations the test pieces were cut in the shape of a dumb-bell and the dimensions in accordance to the requirements described in the standard LST ISO 3376 (length $l_1 = 50$ mm, width $b = 10$ mm). All materials were conditioned at a standard atmosphere 23/50 (temperature $T = 23 \pm 2^\circ\text{C}$, humidity $\varphi = 50 \pm 5\%$) for at least 48 h before cutting in accordance with LST EN 12222. Mechanical tests were carried out with the aid of ZWICK universal testing machine (model Z005 with 5 kN load cell). All tests were conducted at a crosshead speed of 100 ± 10 mm/min under controlled temperature of $23 \pm 2^\circ\text{C}$ and relative humidity of $50 \pm 5\%$. The grip distance was set at 50 mm.

In this article two biaxial deformation methods – membrane (simulation) and punching (experimental) – were applied for the simulation of manufacturing and wearing conditions.

Finite element method (FEM) was used to determine the influence of the stitch number upon the distribution of principal stresses under the membrane (simulation) deformation in leather or PU film layers. Analysis was performed by commercial finite element code COSMOS version 2.5. Multi-layer four-node shell “SHELL 4L” elements with three and four degrees of freedom in each node were used. Anchorage of specimen edges and 1 kN deformation force in the centre of the specimen were used. The generated mesh used for analysis is presented in Fig. 2a. For FEM simulation two different stitch densities were applied, 3 and 5 stitches/cm (Fig. 2b).

Table 1. Mechanical properties of investigated materials

Material and its characterization	Thickness h , mm	Tensile strength σ , MPa	Elongation at break ε , %	Young's modulus E_y , MPa
<i>Elastic Nappa leather</i> : chrome-tanned cowhide leather with pigmented coating	1.25 ± 0.05	11.9 ± 2.1	41 ± 4	36.6
<i>Laminated Permair leather</i> : hybrid leather obtained by hot plate pressing of a separately moulded microporous polymer film (<i>Permair</i> film) to split leather surface using adhesive layer	1.71 ± 0.25	21.9 ± 1.7	37 ± 3	68.8
<i>Microporous polyurethane film</i> : <i>Permair</i> film consisting of interconnected pores with a diameter of 5 μm	0.40 ± 0.05	7.5 ± 0.2	326 ± 14	18.2

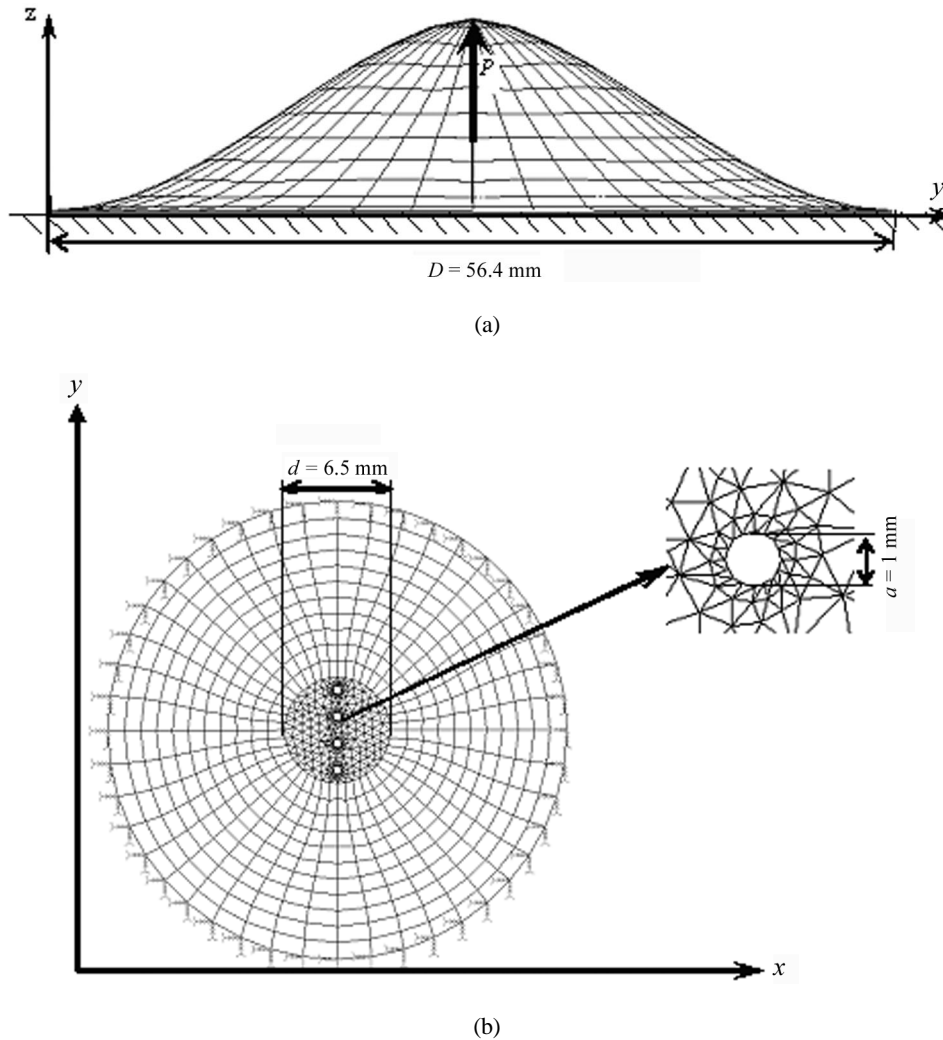


Fig. 2. Generated meshes of shell elements used for finite element simulation under the membrane deformation: (a) general mesh; (b) mesh with modelled stitches.

The calculation algorithm was based on structural geometrical non-linearity, assuming that all components are linear-elastic. In this kind of finite element analysis, the overall stiffness of the structure depends on the stiffness contribution of each of its finite elements. Throughout the history of the load application, the structure is displaced from its original position and the nodal coordinates will change causing the elements to deform and to change their spatial orientations. In small displacement-induced deformations of the element, the change in its spatial orientation is assumed small enough so that the change in its stiffness contribution to the overall structural stiffness can be ignored. On the other hand, in large

displacement analysis the displacement-induced deformations can be finite and local element stiffness will change due to the change in the geometrical shape of the element (length, area, thickness, or volume). Also, the spatial orientation change can no longer be infinitely small, so that the transformation of the local stiffness of the element into global-stiffness contribution will also change. In order to consider the finite change in the geometry of the structures, an auxiliary strain measure, the Green–Lagrange strain tensor, was introduced.

The numerical procedures, which were incorporated in the solution of non-linear problems using the finite element method, were the following:

- control of the computational progress along the equilibrium path (force) of the system;
- an iterative method to solve a set of simultaneous non-linear equations governing the equilibrium state along the path;
- termination schemes to end the solution process.

To use this technique, the pattern of applied loads is proportionally incremented using a single load multiplier to achieve equilibrium under the control of a specified degree of freedom. The controlled degree of freedom is incremented through the use of the “time” curve. The basic set of equations to be solved at any “time” step $t + \Delta t$, is:

$${}^{t+\Delta t}\{R\} - {}^{t+\Delta t}\{F\} = 0, \quad (1)$$

where ${}^{t+\Delta t}\{R\}$ is the vector of externally applied nodal loads and ${}^{t+\Delta t}\{F\}$ is the vector of internally generated nodal forces. Since the internal nodal forces ${}^{t+\Delta t}\{F\}$ depend on nodal displacements at time $t + \Delta t$, ${}^{t+\Delta t}\{U\}$, an iterative method must be used. The following equations represent the basic outline of an iterative scheme to solve the equilibrium equations at a certain time step $t + \Delta t$:

$$\{\Delta R\}^{(i-1)} = {}^{t+\Delta t}\{R\} - {}^{t+\Delta t}\{F\}^{(i-1)}, \quad (2)$$

$${}^{t+\Delta t}[K]^{(i)}\{\Delta U\}^{(i)} = \{\Delta R\}^{(i-1)}, \quad (3)$$

$${}^{t+\Delta t}\{U\}^{(i)} = {}^{t+\Delta t}\{U\}^{(i-1)} + \{\Delta U\}^{(i)}, \quad (4)$$

$${}^{t+\Delta t}\{U\}^{(0)} = {}^t\{U\}, \quad {}^{t+\Delta t}\{F\}^{(0)} = {}^t\{F\}, \quad (5)$$

where ${}^{t+\Delta t}\{F\}^{(i-1)}$ is the vector of internally generated nodal forces, $\{\Delta R\}^{(i-1)}$ is the out-of-balance load vector, $\{\Delta U\}^{(i)}$ is the vector of incremental nodal displacements, ${}^{t+\Delta t}\{U\}^{(i)}$ is the vector of total displacements and ${}^{t+\Delta t}[K]^{(i)}$ is the Jacobian stiffness matrix, all at iteration i .

In the analysis presented here, the Newton–Raphson scheme was used to perform the above iteration, according to which the stiffness matrix is formed and decomposed at each iteration within a particular step. This method has a high convergence rate, which is quadratic. The convergence criterion is based on the

out-of-balance loads during iterations. It requires that the norm of the load vector be within the tolerance ε_f to the applied load increment.

In the case of experimental investigations, a punch forced rounded work zones in the specimens, and the punching strength and elongation at break were determined (Fig. 3a). The punching (experimental test) of the investigated materials was performed using a special punching unit (Fig. 3b). Punches of different radii were used depending on the nature of deformed materials (Table 2). To determine the dependence of the punching strength and elongation at break upon the needle shape and stitch density in the materials, various numbers of oval and rhombus shaped pricks were cut in the direction of the axial line of the leather or PU film specimens. During testing, the specimens were clamped in the tensile testing machine in a way that these pricks were positioned on the axial line of the punch.

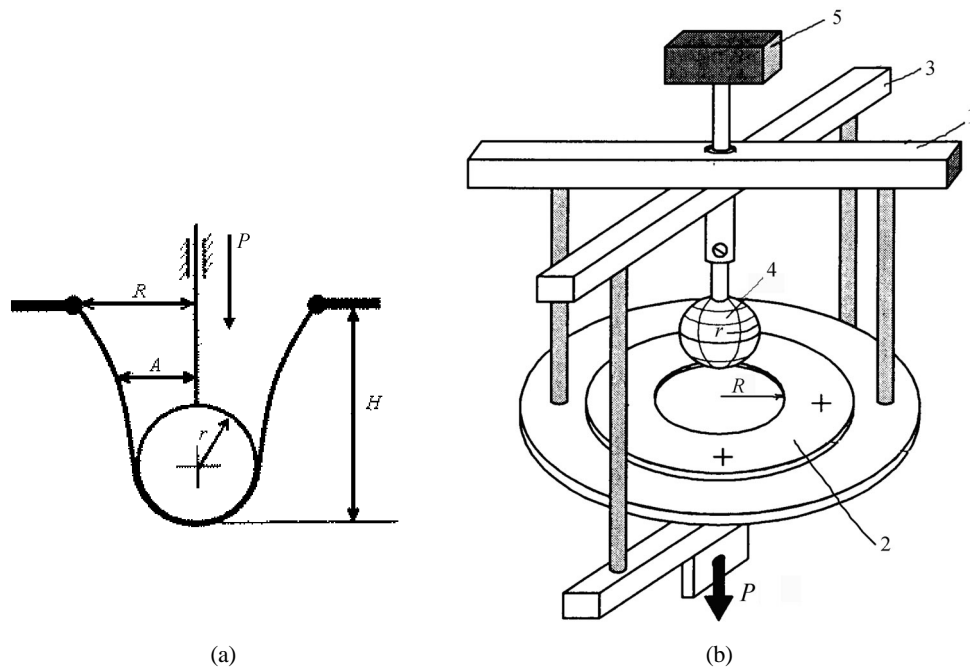


Fig. 3. Punch deformation: (a) principle scheme; (b) punching deformation unit (1 – frame; 2 – clamp of the specimen; 3 – frame of the punch; 4 – punch; 5 – force sensor).

Table 2. Punch and specimen dimensions

Material	Punch radius r , mm	Radius of the work zone of specimens R , mm
Leather, coated or laminated	30	56.4
Microporous PU film	25	40

To determine the influence of the shape and number of the prick on the punching strength and elongation at break, square specimens of 140×140 mm were obtained. Five circles, the radius of which varied by the step of $\Delta = 10$ mm, were drawn at the centre of specimens (as seen in Fig. 6). The stitches of various shapes (oval and rhombus) were made in the centre line of specimens in the longitudinal direction of the material.

Before testing, all specimens were conditioned for at least 48 h in a standard atmosphere 23/50 in accordance with EN 12222:1997.

3. RESULTS AND DISCUSSIONS

In Fig. 4 typical stress-strain curves of the pigment coated leather, laminated leather and microporous PU film are presented. They were found to be different depending on the material nature. The stress–strain relationship of leather was slightly non-linear. For pigment coated leather, the tensile strength increased linearly approximately up to 15 MPa. It had initial Young’s modulus of about 51 MPa and elongation at break of 58%. Microporous PU film exhibits typical elastomeric behaviour with tensile strain up to 350%. However, no obvious necking occurs with low ultimate tensile strength (only 7.5 MPa).

The lamination of split leather by the microporous PU film improves tensile properties of the hybrid leather. The tensile strength has been increased up to 23 MPa. Young’s modulus also increases up to 69 MPa. However, the lamination practically does not improve the strain properties of leather. Besides, the differences in tensile properties of the laminated leather can be related not only to the finishing procedure, but also to initial properties of the sample, zone of the leather, defects, etc. [10].

Stress distribution in the leather of various finishing techniques and PU film for numbers of stitches 3 and 5 cm^{-1} under membrane deformation is presented in Fig. 5.

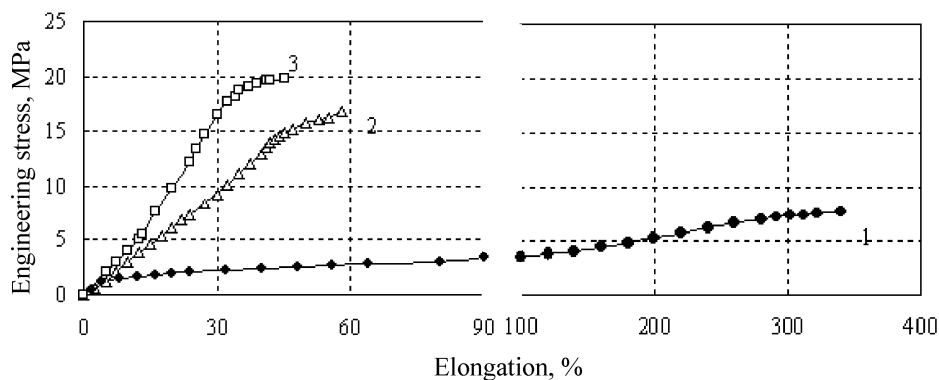


Fig. 4. Stress-strain curves for microporous PU film (1), pigment coated leather (2) and laminated leather (3).

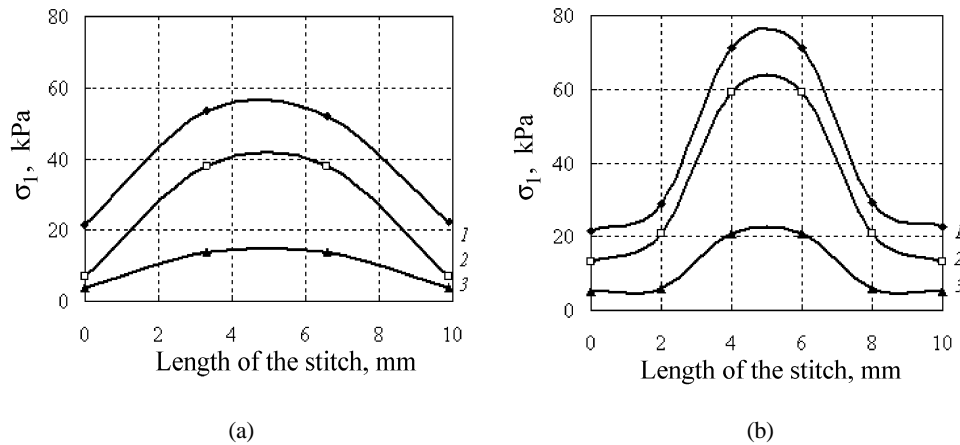


Fig. 5. Dependence of σ_1 on the length of the stitch during membrane deformation for different numbers of stitch: (a) 3 cm^{-1} ; (b) 5 cm^{-1} ; 1 – laminated leather; 2 – pigment coated leather; 3 – PU film.

According to FEA data it is evident that the principal stress distribution in leathers depends not only on the stitch density, but also on the prick shape. The nature of the material also has an influence on the stress distribution.

Stresses reach the maximal value in the middle of the stitch. In this area stress value is higher about four to five times compared to that in the beginning or in the end of stitch. The highest stress is developed in the laminated leather. In the case of stitch density of 3 cm^{-1} , principal stress reaches maximal value of 53 kPa (in the pigment coated leather 38 kPa and in the polyurethane film 14 kPa).

Increase of the stitch density up to 5 cm^{-1} increases stress during membrane deformation. In this case also the highest stress appears in laminated leather and the lowest in the polyurethane film. Stress value increases up to 71 kPa in laminated leather, whereas in polyurethane film up to 21 kPa.

Further it was interesting to investigate the behaviour of the laminated leather upon the shape and distribution of the stitch under punching deformation. A significant factor, affecting the character of breaking of the materials during punch testing, is friction between the specimen and the punch. Because of it, maximal stresses are located at the contour line where the specimen loses its contact with the punch. For materials such as leather, with slight anisotropy, the breaking line has an indefinite shape or forms a “ring” [11]. In the case of membrane deformation simulation no friction exists, and due to this maximal stresses appear at the corner of the pricks in the direction of lowest strength or lowest deformation of the material.

During punching [12], stress is concentrated at the shell top. Notwithstanding the materials breakup below supposed line. The investigations show that independent of the nature of the material, the breaking line is straight below the specimen and punch contact zone. As can be seen from Fig. 6, in the case of a punch with a

radius of 30 mm the breaking line of the PU film laminated leather is located practically at the distance, which is approximately equal to the punch radius.

The crack formation and propagation during punching changes when the needle pricks of different shape and number were made in the leather or PU film. From Fig. 7 it is evident that for pigment coated leather the punching strength is considerably higher (1300–1600 N) compared to that of the PU film (200–300 N). It can be also mentioned that punching strength of laminated leather reaches very high values, up to 4000–5000 N.

Besides, punching strength slightly depends upon prick shapes when their density is low (especially for oval pricks). It may be supposed that pricks increase the deformation of the leather and the work involved for its deformation also increases. Meanwhile, the rhombus shaped pricks at higher densities decrease the punching strength of leather due to the formation of defect zones with high stress concentration. In the case of the PU film the punching strength decreases monotonically with the increase of the number of pricks.

Further investigations showed that crack formation and propagation in pigment coated leather also depends on the prick shape and density. In the case of 1 or 3 pricks, independent of their shape, cracks form in the corner of the prick and propagate in the direction of lowest deformation. While in the case of 5 pricks, breakup of leather specimen depends upon the prick shape. As investigations of membrane deformation show, in the case of rhombus shaped prick, for which higher stressed regions are characteristic, crack location and its propagation direction does not change. However, in the case of oval prick the leather breakup occurs in the line of pricks, independent of the anisotropy of the material. Thus at the higher prick density leather breaking behaviour does not depend upon the prick shape.

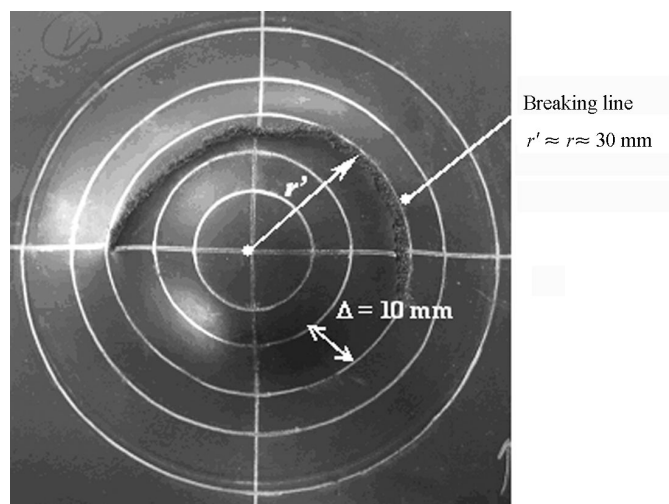


Fig. 6. Breaking scheme of the laminated leather after punching.

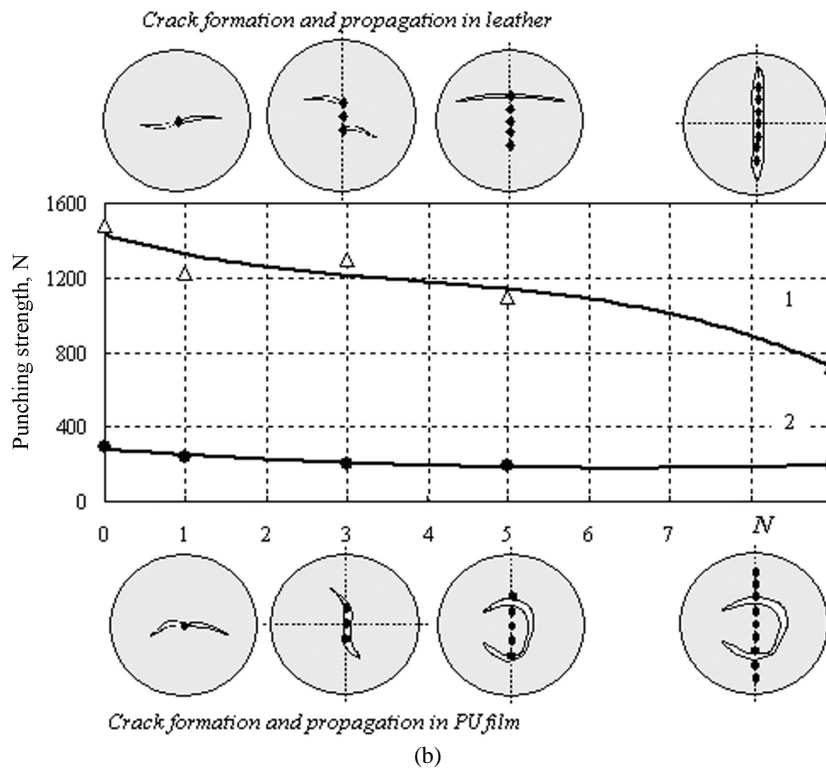
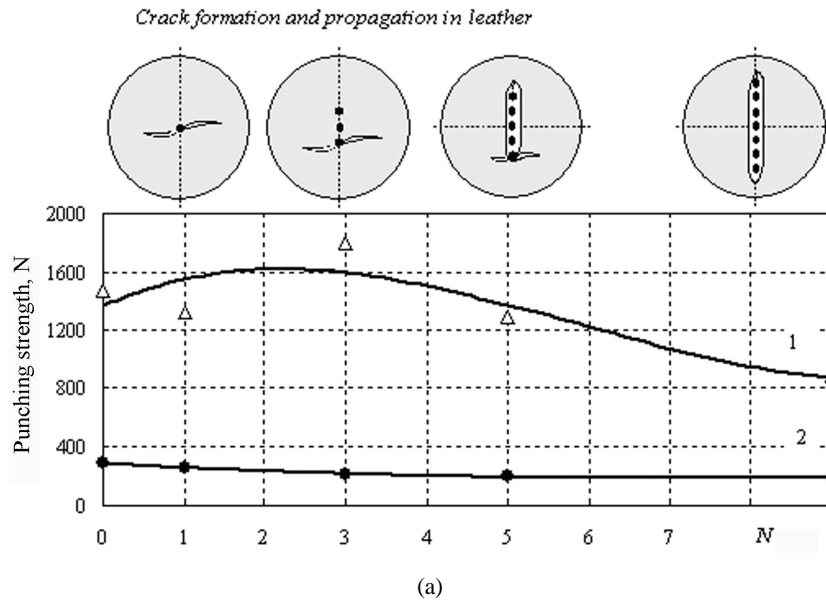


Fig. 7. Dependence of the punching strength and crack formation and propagation upon the shape and number of needle pricks: (a) oval prick; (b) rhombus prick; 1 – pigment coated leather; 2 – PU film (N – number of pricks).

On the other hand, the prick shape does not influence the breaking character of the PU film. Thus, in the case of one prick, the crack propagates perpendicularly to the direction of highest deformation. Higher prick density influences the breaking character. In the case of 3 pricks, crack propagates in the direction of the lowest deformation, but breakup in the line of pricks also occurs. The increase of pricks up to 5 or more determines the formation of the ring shaped break line below the contact zone of the specimen and punch.

It should be mentioned that crack formation in the PU film laminated leather has the same character as in pigment coated leather. So, it may be supposed that deformation character of the laminated leather with simulated pricks is mainly determined by the properties and structure of split leather but not by the characteristics of the PU film.

The influence of the prick shape and density upon the elongation at break under punching is presented in Fig. 8. As it can be seen, elongation at break of the PU film practically does not depend on the prick shape and their number up

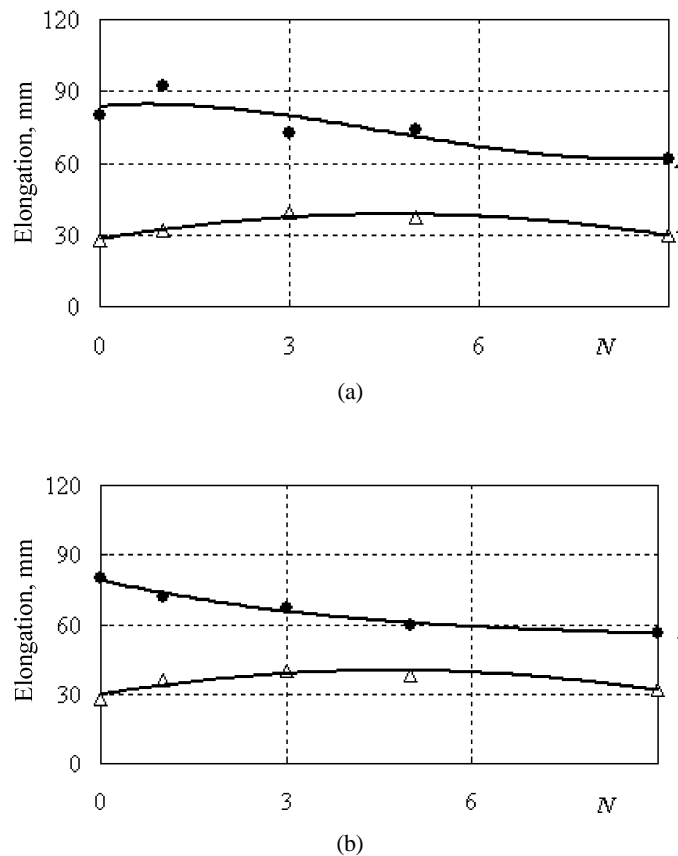


Fig. 8. Dependence of the elongation at break on the shape and number of pricks N : (a) oval prick; (b) rhombus prick; 1 – pigment coated leather; 2 – PU film.

to 5. Further increase of the prick number decreases the PU film elongation by break at 30% in the case of the oval prick and at 22% when the rhombus shaped prick is applied.

The elongation at break under punching of pigment coated leather slightly increases from 28 up to 39–40 mm, when prick number increases up to 5. It should be mentioned that leather elongation at break does not depend on the prick shape. Further increase of the prick density determines marginal decrease of the elongation at break of the leather specimens (down to 30–32 mm).

Thus investigations show that needle and stitch parameters considerably influence the mechanical behaviour of leather and microporous polyurethane film.

4. CONCLUSIONS

The needle and stitch parameters have a significant influence on pigment coated and polymeric film laminated leather and polyurethane film behaviour under biaxial loading. Needle shape, stitch density and the nature of the stitched material significantly influence the principal stress distribution in leathers and PU film during membrane deformation. Stresses reach their maximal values in the middle of the stitch. Stress concentration increases as stitch density increases.

Investigations of the influence of the needle and stitch parameters on mechanical properties of leathers and polyurethane films during punching show that crack formation and propagation during punching depend upon the nature of the investigated materials and on the shape of pricks. It was shown that the strength of materials is higher when prick is oval shaped. The punching strength and elongation of the leather at break slightly increases when prick density is low. Punching strength of PU film decreases as prick density increases.

A significant factor, affecting the character of the breaking of the materials during punch testing, is friction between the specimen and the punch. Because of it, maximal stresses appear at the contour line where the specimen loses its contact with the punch. In the case of membrane deformation simulation no friction exists and due to this maximal stresses appear in the corner of the pricks.

REFERENCES

1. Thorstensen, T. C. *Practical Leather Technology*, 4th ed. Shoe Trade Publishing, New York, 1993.
2. Satas, D. and Tracton, A. A. *Coatings Technology Handbook*, 2nd ed. Marcel Dekker, New York, 2001.
3. Sarkar, K. T. *Retanning, Dyeing and Finishing of Leather*. Shoe Trade Publishing, New York, 1996.
4. Gibson, P. W. Effect of temperature on water vapor transport through polymer membrane laminates. *Polym. Test.*, 2000, **19**, 673–691.
5. Tuckermann, M., Mertig, M., Pompe, W. and Reich, G. Stress measurements on chrome-tanned leather. *J. Mater. Sci.*, 2001, **36**, 1789–1799.

6. Rajini, K. H., Usha, R., Arumugam, V. and Sanjeevi, R. Fracture behaviour of cross-linked collagen fibres. *J. Mater. Sci.*, 2001, **36**, 5589–5592.
7. Milašienė, D., Jankauskaitė, V. and Arcišauskaitė, A. Prediction of stress relaxation in laminated leather layers. *Materials Science (Medžiagotyra)*, 2003, **9**, 73–79.
8. Milašienė, D. and Jankauskaitė, V. Comparable evaluation of methods of stress relaxation prediction in leather. *Mechanika*, 2003, **4**, 11–18.
9. Lang, Sh. Y. T., Rao, K. P. and Ching, L. T. Mechatronic design of a leather spray system. *Mechatronics*, 1999, **9**, 867–880.
10. Rajini, K. H., Usha, R., Arumugam, V. and Sanjeevi, R. Fracture behaviour of cross-linked collagen fibres. *J. Mater. Sci.*, 2001, **23**, 5589–5592.
11. Tijiūnienė, L., Strazdienė, E. and Gutauskas, M. The behaviour of polyethylene membrane due to punch deformation process. *Polym. Test.*, 1999, **18**, 635–640.
12. Ogden, R. W. *Non-Linear Elastic Deformation*. Wiley, New York, 1984.

Pingete jaotus polümeerkilega kaetud nahas kahesuunalise koormuse korral

Virginija Jankauskaitė, Eugenija Strazdienė ja Agnė Laukaitienė

On uuritud nõela ja piste parameetrite mõju pigmendiga töödeldud ja polümeerkilega kaetud parknaha käitumisele kahesuunalisel koormamisel. Nahka on mulgustatud spetsiaalse stantsi abil, pistete arvu mõju pingetele on analüüsitud ka lõplike elementide meetodil. On leitud, et pinged pistete keskosas on 4–5 korda suuremad kui otstes ja kasvavad pistete tihenedes. Nahk ja poliüuretaankile katkevad otse proovi ja stantsi kokkupuutetsooni all. Pragude teke ja levik sõltuvad pistete tihedusest ja nõela kujust.